Adrenergic activation of cardiac preganglionic neurons in nucleus ambiguous relies on persistent sodium current

Isamu Aiba and Jeffrey L. Noebels
Department of Neurology, Baylor College of Medicine Houston TX 77030

Running title: Adrenergic activation of vagal neurons

Key words: Nucleus ambiguus, parasympathetic, cardiac vagal neurons, persistent sodium current, adrenergic signaling, T-type calcium current

Key points summary

- In the ventral medulla, Nucleus ambiguus (NAm) contains cardiac preganglionic cholinergic neurons responsible for parasympathetic regulation of cardiac pacemaking.
- Adrenergic agonists potently activate the cardiac neurons, elevate membrane resistance, and generate rhythmic activity in otherwise quiescent cholinergic NAm neurons in acute brainstem slices.
- Adrenergic activation does not require synaptic transmission, but relies upon changes in intrinsic membrane excitability.
- Various pacemaker currents, such as hyperpolarization activated current (Ih), T-type calcium current (ICaT) and persistent sodium current (INaP) are expressed in these neurons, however only INaP is a critical contributor.

- These results demonstrate a potent and hitherto unknown non-synaptic depolarizing membrane mechanism of adrenergic agonists on cholinergic NAm neurons. The modulatory influence of adrenaline on central parasympathetic outflow contributes to homeostatic balance of both physiological and deleterious cardiovascular regulation.

Abstract

Cardiac parasympathetic control is mediated by cholinergic vagal nerve fibers projecting from neurons in the brainstem nucleus ambiguus (NAm). Central adrenergic signaling modulates this output; however the exact excitability mechanisms are not fully understood. We investigated responses of NAm neurons to adrenergic agonists using *in vitro* mouse brainstem slices. Preganglionic NAm neurons were identified by Chat-tdtomato fluorescence in young adult transgenic mice (P20-50) and their cardiac projection confirmed by retrograde dye tracing. Juxtacellular recordings detected spontaneous action potentials (AP) in NAm neurons. Bath application of epinephrine or norepinephrine strongly and reversibly activated most NAm neurons regardless of basal firing rate. Epinephrine was more potent than norepinephrine, and pharmacological analysis confirmed that activation utilized α1 and β-type adrenoceptors. Interestingly, adrenergic activation of NAm neurons does not require a presynaptic mechanism, since receptor blockade did not fully occlude the excitatory effect, and epinephrine did not alter tonic excitatory or inhibitory synaptic transmission. Instead, adrenergic agonists significantly elevated intrinsic membrane excitability, leading to prolonged recurrent rebound action potentials in response to a brief hyperpolarization pulse. T-type calcium current (ICaT), but not hyperpolarization-activated current (Ih), partially contributed to the excitability increase. However pharmacological blockade of persistent sodium current (INaP) with riluzole fully prevented the high intensity adrenergic discharge. Our results demonstrate that central adrenergic signaling enhances the intrinsic excitability of NAm neurons, and persistent sodium current plays a predominant role in this effect. This central balancing mechanism may counteract excessive peripheral cardiac excitation during increased sympathetic tone.

Introduction

Central parasympathetic autonomic regulation is predominantly mediated by vagal preganglionic fibers originating in the ventrolateral brainstem medulla oblongata. The caudal portion of the nucleus ambiguus (NAm) contributes the majority of axons in the cardiac vagus nerve and is responsible for cholinergic reduction of heart rate. Chronically reduced vagal tone is implicated in an increased risk of ventricular tachycardia and fibrillation, while enhanced tone has antiarrhythmic properties (Kalla, Herring et al. 2016). On the other hand, acute vagal hyperactivity may lead to bradycardia, asystoles, atrial fibrillation, vagal reflex syncope and, in severe cases, cardiac arrest (Colman, Nahm et al. 2004; Alboni, Alboni et al. 2011). Strong autonomic co-activation is also arrhythmogenic and evokes complex sympathetic- and parasympathetic-driven cardiac arrhythmias (Koizumi and Kollai 1981), which can be life-threatening in people with heart disease (Shattock and Tipton 2012).

Central adrenergic signaling is likely involved at several levels in homeostatic responses to stress autonomic regulation (Kvetnansky, Sabban et al. 2009). The descending adrenergic neurons within the rostral ventrolateral medulla brainstem (e.g. A5, C1r groups) project to preganglionic cardiac sympathetic neurons in the intermediolateral cell column of the thoracic spinal cord to modulate cardiac sympathetic outflow (Loewy, McKellar et al. 1979), and subsets of these adrenergic neurons may also project collaterals to Nam (Kalia, Fuxe et al. 1985; Byrum and Guyenet 1987; Stocker, Steinbacher et al. 1997) to modulate vagal outflow (Abbott, DePuy et al. 2013). Adrenergic neurons in the locus coeruleus (A6 group) neurons also modulate local inhibitory synaptic transmission in the NAm (Wang, Pinol et al. 2014). Given the need to maintain tight coordination for optimal sympathetic and parasympathetic balance, central adrenergic feedforward signaling may play important roles in determining cardiac autonomic regulation. However the mechanisms underlying adrenergic signaling onto preganglionic neurons in the NAm is not fully understood. Synaptic activation of NAm neurons is regulated by ionotropic glutamate, GABA and glycine signaling, and this input is influenced by various neuromodulators (Jameson, Pinol

et al. 2008; Dergacheva, Kamendi et al. 2009; Philbin, Bateman et al. 2010; Dyavanapalli, Byrne et al. 2013; Sharp, Wang et al. 2014; Dergacheva, Yamanaka et al. 2016). The intrinsic membrane excitability of NAm neurons is also sensitive to neuromodulators, for example, aldosterone in neonatal rat neurons (Brailoiu, Benamar et al. 2013). However, the relative importance of synaptic versus intrinsic membrane excitability mechanisms to the discharge patterns of NAm neurons has not been fully explored, nor is it known whether mechanisms studied in immature animals are conserved in the young adult (Kasparov and Paton 1997).

This *in vitro* study of young adult Nam cholinergic neurons in mouse brainstem slices shows that adrenergic agonist exerts potent non-synaptic excitatory effects on preganglionic vagal neurons. In the presence of synaptic receptor blockade, adrenergic agonists reliably increased the spontaneous AP discharge rate of NAm neurons. This excitatory effect produced a robust rhythmic discharge pattern that did not depend upon low threshold T-type calcium current or Ih current, but rather potentiated intrinsic membrane excitability by engaging non-inactivating sodium currents, since it was prevented by selective blockers of prolonged inward sodium current. This previously unidentified mechanism may play an important role in coordinate regulation of sympathetic and parasympathetic autonomic system, and may be a useful target for treatment of abnormal cardiac conditions.

Material and methods

Animals

All experiments were conducted under the protocol approved by the IACUC at Baylor College of Medicine. Chat-IRES-cre mouse (JAX: stock No: 006410) and floxed tdtomato

gene (Ai9, JAX: Stock No: 007909) were obtained from Jackson laboratory and crossed to generate Chat-cre (+/-), tdtomato (+/- or +/+) mouse line. Mice at age between P20-45 with both sex were used.

Retrograde labeling of cardiac premotor neurons in brainstem

Mice (Chat-cre, tdtomato) were deeply anesthetized with avertin (Tribromoethanol, 200 mg/kg i.p.) or 2% isoflurane. Skin overlying the precordial region was depiliated, cleansed, and a small vertical skin incision made along sternal line. The thoracic wall was exposed and DiO suspension (30 mg/ml, 100 µl, 30% DMSO in saline) was slowly injected into the pericardial space via the intercostal spaces of the left 3-5th ribs (~1.5 mm depth). Breathing pattern was carefully monitored to ensure absence of pneumothorax. The skin incision was sutured and the mouse allowed to recover for at least 1 week. For histological analysis, mice were cardiac-perfused with ice cold PBS followed by 4% PFA. Brain was extracted and kept in 4% PFA for overnight at 4°C, followed by further incubation in 30% sucrose until brain sinks. Brain was embedded in OCT compound and cut in 50-70 µm coronal sections with a cryostat. Brain sections were rinsed with PBS, mounted on slide glass. Fluorescence images were acquired on a fluorescence microscopy (Nikon TE2000S) with NIS element program and analyzed with imageJ program.

In vitro Electrophysiology

Mice were deeply anesthetized with avertin (Tribromoethanol, 200 mg/kg i.p.), cardiac perfused with a brain cutting solution (in mM: 110 NMDG, 6 $MgSO_4$, 25 $NaHCO_3$, 1.25 Na_2HPO_4, 3 KCl, 10 glucose, 0.4 ascorbate, 1 thiourea, saturated with 95% O_2/5% CO_2) and decapitated. The brain was quickly extracted in ice-cold cutting solution, the isolated hindbrain was glued to a mold, cerebellum removed and 200 µm thick coronal medulla slices were cut with a vibratome (Leica VT-1200). Slices were further hemisected at the midline, incubated in ACSF (in mM: 130 NaCl, 3 KCl, 25 $NaHCO_3$, 1.25 Na_2HPO_4, 10 glucose, 0.4 ascorbate, saturated with 95% O_2/5% CO_2) at 32°C for 1 hour, then kept in oxygenated ACSF at room temperature.

Recordings were made in a submerged chamber (RC27, warner instruments) continuously perfused with ACSF at 2.5ml/min and 32-33°C. NA was visually identified in the transparent regions located in ventral medulla, and the cholinergic neurons were confirmed by presence of tdtomato fluorescence. Whole-cell recordings were made on visually identified tdtomato+ neurons. All electrophysiological signals were amplified with a Multiclamp 200B amplifier, digitized and acquired with Clampex software (Molecular Devices). Data were analyzed with pClamp9 and Mini Analysis Program (Synaptosoft).

Cell attached patch recordings were made by voltage clamp recording with micro pipettes containing ACSF. Seal resistance was between 5-50 MΩ. Data were >1 Hz high pass filtered. In order to minimize perturbation of membrane potentials of recorded neurons, the command voltage was adjusted to a voltage at which holding current was within ±300 pA (Perkins 2006). Recordings were included for analysis only when neurons showed spontaneous action potentials, or silent at rest but with action potentials that could be evoked by bipolar stimulation (electrodes ~300 µm apart) of adjacent tissue.

In whole cell recordings, the membrane resistance, capacitance and access resistance were determined using the membrane test protocol of Clampex software (+20 mV, 20 ms rectangular test pulse, at -60mV holding potential). Data were >100 Hz low pass filtered. Cells with an access resistance <20 MΩ were accepted for analysis.

Current clamp recordings were made with potassium gluconate internal solution (in mM: 135 potassium gluconate, 10 HEPES, 1 $MgCl_2$, 8 NaCl, 0.05 EGTA, 2 Mg-ATP, 0.3 Na-GTP, pH adjusted to 7.2 with KOH). Intrinsic membrane excitability was tested after adjustment of bridge balance. Responses to rectangular test pulses (-200 to +450 pA, 50 pA increment, 500 ms) were measured at resting potential or -60mV to avoid generation of spontaneous action potentials.

Voltage-clamp recordings were made with a cesium gluconate internal solution (in mM: 130 gluconic acid, 10 HEPES, 1 $MgCl_2$, 8 NaCl, 10 BAPTA, 5 TEA, 5 QX314, 2 Mg-ATP, 0.3 Na-GTP, pH adjusted to 7.2 with CsOH). Liquid junction potentials were adjusted by -10 mV. Low voltage-activated currents were evoked by the following current protocol: prepulse at -110 mv for 2 seconds followed by voltage step to various potentials (-70 to -30mV with 10mV increment). Maximum current amplitude was obtained from the

activation curves. When testing steady state inactivation (SST), T-type calcium current was evoked with hyperpolarizing prepulses (-110 to -50 mV with 10 mV increments) at 2 second intervals, followed by an activation voltage step to -50 mV. Both activation and SST I-V curves were fitted to a sigmoidal curve and V_{50} values were calculated. Persistent sodium current was recorded with a cesium gluconate internal solution without sodium channel blocker QX314. Cadmium (100 µM) was included in the superfusate to reduce voltage-gated calcium currents. Neurons were clamped at -80mV and slowly depolarized by a voltage ramp (20 mV/s) until +20 mV. After obtaining basal current, recordings were repeated in the presence of tetrodotoxin (TTX: 10 nM, 1 µM) or 30uM riluzole to isolate the INaP component. Traces averaged from 3-6 sweeps were used for analysis.

Drugs

Epinephrine, norepinephrine, phenylephrine, doxazosin were from Sigma Aldrich USA. NBQX, gabazine (SR 95531), carveninolol and riluzole were obtained from Tocris. TTPA2 and TTX were purchased from Alomone Labs. Riluzole was dissolved in DMSO at 300 mM and stored at -20°C. Other drugs were directly dissolved in ACSF on the day of experiments. The selective T-type calcium channel blocker Z944 was kindly provided by Dr Terry Snutch (Tringham, Powell et al. 2012).

Results

Putative cardiac premotor neurons in the nucleus ambiguus (NAm)

Preganglionic neurons in the nucleus ambiguus (NAm) were identified using a transgenic mouse which expresses tdtomato fluorescent protein under the control of the *choline acetyl transferase* (Chat) promoter (Chat-tdtomato). Their cardiac projection was verified by retrograde labeling with a tracer dye (DiO) injected into the pericardial sac (see methods) **Figure 1A.** All retrogradely labeled DiO^+ cells were tdtomato positive and had a large soma diameter (>40 µm), while ~10% of the Chat-tdtomato$^+$ cells were not labeled with

retrograde tracers. These non-cardiac labeled cells had smaller somata and were sparsely distributed within and around the NAm (**Figure 1B**) n=3 mice).

The electrophysiology of Chat-tdtomato$^+$ cells was further characterized *in vitro* using acute slices prepared from young adult (P20-P50) mouse brainstem. The two populations with different cell sizes could be also distinguished *in vitro* and showed distinct electrophysiological properties. Consistent with the difference in soma size, these two populations had different mean membrane capacitances (90.9±19.4 pF vs 36.6±4.4 pF, n=100, 9, **Figure1D**). The resting potentials were similar (-54.5±5.4 mV vs -54.1±1.5 mV **Figure1E**). The membrane resistance of neurons with larger soma diameter was relatively homogenous, while membrane resistances of the smaller neurons were highly variable (130.0±53.8 MΩ vs 663.4±382.0 MΩ, **Figure 1F**). These results suggest that the Chat-tdtomato$^+$ cells with a small soma are a mixed population and may be cholinergic local circuit or oropharynx/larynx projection neurons (Irnaten, Wang et al. 2001). Based on histology and electrophysiological characterizations, the Chat-tdtomato$^+$ cells with larger soma (>40 µm diameter) are presumed to be the long range cardiac preganglionic neurons, and in subsequent experiments, all analyses were made from this cholinergic neuron group.

Adrenergic agonists activate spontaneous rhythmic AP firing in NAm neurons in part via α1 and β receptor mechanisms

Adrenergic signaling plays an important role in central autonomic control of NAm cholinergic output by modulating excitatory and inhibitory synaptic transmission, as shown by subtype selective adrenoceptor agonists/antagonists (Philbin, Bateman et al. 2010; Boychuk, Bateman et al. 2011; Bateman, Boychuk et al. 2012; Sharp, Wang et al. 2014). In these studies, the effects may be due to altered neurotransmitter release at afferent presynaptic terminals, however the possibility of direct postsynaptic effects has not yet been clearly demonstrated. We recorded NAm AP firing using cell-attached microelectrode recordings. Under basal conditions, NAm cells showed a variety of spontaneous AP firing patterns in vitro, ranging from complete silence to active firing

(2.14±2.60 Hz, n=79 neurons, **Figure 2C**). Bath application of epinephrine (hereafter Epi; 10 μM) or norepinephrine (hereafter NE; 10 μM) significantly enhanced spontaneous AP firing in NAm neurons (**Figure 2A**). Epinephrine increased the spontaneous action potential rate in a majority of these cells (90% (71/79 cells)), while the remainder (10%; 8/79 cells) displayed a 'burst suppression' firing pattern (**Figure 2B**). Due to the low chance of encountering the burst cells, further characterization focused on the regular-spiking cells.

Epi had a stronger modulatory effect than NE. Repetitive agonist exposure and washout experiments showed that Epi increased spontaneous AP rate 9.7±1.4 fold, while NE increased AP 2.1±0.9-fold in the same neurons (n=7, Figure 2D). Due to its higher efficacy, the majority of subsequent experiments were performed using epinephrine as an agonist.

We next examined the adrenoceptors involved in adrenergic NAm activation. In order to ensure regular-spiking response to Epi, NAm neurons were first exposed to Epi, washed, and then re-exposed to Epi with a selective antagonist. In the experiment shown, neurons that responded to Epi by increasing their AP firing rate were analyzed. The pan-β receptor antagonist propranolol (10 μM) strongly attenuated the basal spontaneous AP firing rate (75.7±31% reduction), and prevented AP increases in 40% (2/5) of cells tested (**Figure 3A**). Likewise, the α1 antagonist doxazosin reduced basal AP rate by 92.8±11.8% and prevented AP induction in 86% (6/7) neurons (**Figure 3B**). In the reverse experiment, bath application of the α1 agonist (10-50 μM), phenylephrine (PE), induced a spontaneous AP discharge in 50% (4/8) of NA cells (**Figure 3C**). Finally, carvedilol, a dual α1- and β- blocker, also reduced basal AP rate by 74.2±23.7%, and prevented an Epi-dependent AP increase in 80% (4/5) cells and severely attenuated the induction in a remaining cell (1/5 cell) (**Figure 3D**). These results suggest that activation of both α1- and β-receptors are involved in direct epinephrine-dependent NAm activation. Reduction in the basal firing rate by the antagonists also suggests that endogenous adrenergic signaling maintained the tonic spontaneous AP firing of NAm neurons in our preparation.

AP induction by adrenergic agonist occurs independently of synaptic input

Subtype selective adrenergic agonists/antagonists have been shown to modulate synaptic transmission in cardiac vagal neurons within NAm recorded in neonatal rat brainstem slices (Philbin, Bateman et al. 2010; Boychuk, Bateman et al. 2011; Bateman, Boychuk et al. 2012; Sharp, Wang et al. 2014; Wang, Pinol et al. 2014). We examined whether such synaptic modulation fully explains the adrenergic activation seen in NAm neurons studied in our preparation from young adult mouse. Bath application of NBQX (10 µM), the AMPA/kainate receptor antagonist, significantly decreased AP discharge rate of spontaneously active NAm neurons (58.8±40.4% decrease, n=6, **Figure 4A**), however Epi still increased the AP firing rate in 89% (8/9) of the regular spiking NAm neurons tested (**Figure 4A**). These results indicate that tonic glutamate receptor activation supports the spontaneous activity of NAm neurons, but is not required for AP induction by adrenergic agonists. We also tested whether inhibitory control was similarly affected, by eliminating inhibitory synaptic currents using co-application of a mixture of the $GABA_AR$ antagonist gabazine (10 µM) and the GlycineR antagonist strychnine (1 µM). This synaptic disinhibition did not significantly modulate the basal spontaneous AP rate (5.7±22.3 % decrease, n=4 cells **Figure 4B**), and Epi still increased the spontaneous AP rate in all neurons tested (100%, 4/4 cells, **Figure 4B**). These results demonstrate that adrenergic activation of NAm neurons does not rely solely on either excitatory or inhibitory synaptic transmission

To further examine whether NAm activation by adrenergic agonists might include a presynaptic component, postsynaptic currents of the NAm neurons were recorded during Epi or NE exposures. The isolated sEPSC and sIPSC currents were effectively blocked by NBQX (10 µM) and gabazine (10 µM)/ strychnine (1 µM) mixture, respectively (**Figure 4C, D**). Exposure to 10µM Epi or NE, which reliably modulated AP firing of the NAm neurons, had no effect on the sEPSC or sIPSC frequency (**Figure 4E, F**). Thus there is no change in spontaneous synaptic transmission induced by adrenergic agonists at a concentration sufficient to increase the spontaneous AP firing rate of NAm neurons. Together these results suggest that although spontaneous synaptic transmission onto NAm neurons contributes to their spontaneous discharge, it is not critically required for adrenergic activation of NAm neurons, at least in isolated *in vitro* slices.

Modulation of intrinsic membrane excitability by adrenergic agonists

We next examined whether modulation of intrinsic membrane excitability could be a potential contributor to the adrenergic activation of NAm neurons. We characterized excitability of NAm neurons by whole-cell recordings. Similar to previous studies (Johnson and Getting 1991; Johnson and Getting 1992), depolarizing current evoked a train of regular APs interleaved with a large immediate after-hyperpolarization likely mediated by SK channels (Lin, Hatcher et al. 2011). A brief hyperpolarizing current typically accompanied by a membrane sag and followed by a rebound AP immediately after termination of hyperpolarizing current was seen in 88% of neurons (88/100 cells, **Figure 5A**). There was variability in the rebound AP shape during a spike train; one showing an immediate small afterhyperpolarization (e.g. **Figure 5A**) can be contrasted with another with a larger after-hyperpolarization (e.g. **Figure 5B**). In both cases, the rebound depolarization was highly sensitive to intracellular dialysis and became undetectable within ~3 minutes after the membrane break-in (**Figure 5A**). This rundown could be partly prevented when 0.5-1 mM spermine was supplied in the intracellular solution (**Figure 5B**), suggesting that endogenous polyamines or related molecules actively maintain excitability (see Discussion). Spermine (0.5 mM) was therefore routinely included in the subsequent whole-cell current clamp recordings.

Bath application of Epi and NE significantly modified intrinsic excitability of NAm neurons (**Fig 5C-E**). A representative response is shown in Figure 5C. Consistent with extracellular recordings, Epi exposure triggered continuous spontaneous discharges in whole-cell recorded NAm neurons when held at -50mV. In order to avoid spontaneous AP generation, intrinsic membrane excitability was determined at -60mV. As shown in Figure 5D and E, Epi exposure significantly modulated excitability of NAm neurons. Epi and NE always increased membrane resistance by 24.9±11.4% (n=10) and 17.7±16.0% (n=13), respectively, while no changes were seen in control experiments (-15.4±21.6%, n=7, **Figure 5F**). This was accompanied by a larger membrane sag during hyperpolarization

mediated by Ih current, and enhancement of rebound depolarization which frequently resulted in AP generation mediated by T-type calcium channels, even at -60mV (see below). The change in rebound AP was robust and a single brief hyperpolarization pulse (<500 ms) could evoke recurrent AP firing lasting 3-5 seconds (see **Figure 7C**). On the other hand, Epi and NE did not change the numbers of AP evoked by depolarizing current pulses (**Figure 5G**). Overall, these adrenergic agonists selectively increased some but not all aspects of intrinsic membrane excitability.

Ih- current in NA neurons

The voltage-sag observed during hyperpolarization indicates the presence of hyperpolarization-activated current (Ih) current, and a previous study in guinea pig suggested that cesium-sensitive Ih current (Q-current) is involved in rebound depolarization of NAm neurons (Johnson and Getting 1991). Ih is required for spontaneous AP generation in various neurons (Resch, Fenselau et al. 2017), however this was not the case in the NAm. We found that the selective Ih inhibitor ZD7288 completely abolished the voltage sag (n=3 **Figure 6A**), however under this condition, epinephrine remained effective at inducing AP firing in all NAm neurons tested (n=3, **Figure 6B**). Thus Ih is functionally expressed in Nam cholinergic neurons, but is not required for adrenergic activation of these cells.

T-type calcium current in NA neurons

T-type calcium channels are expressed in various pacemaking cells and contribute to spontaneous AP discharges (Chemin, Monteil et al. 2002; Perez-Reyes 2003). We next examined the potential role of T-type Ca^{2+} current (ICaT) in NAm excitability. In voltage clamp recordings, low voltage activated current was reliably evoked by a voltage protocol with a mean current density 4.90±1.28 pA/pF (**Figure 7A**), a half-activation voltage of -54.63±1.24 mV and a half-maximum steady stationary inactivation of -77.56±0.63mV (**Figure 7B**). The ICaT inhibitors TTP-A2 and Z944 (1 µM, n=2 for each drug) abolished the inward current as well as the generation of rebound AP's in both control solution and following Epi exposure (**Figure 7C**). The ICaT significantly contributes to NAm excitability, since the inhibitor Z944 reduced the spontaneous AP discharge rate by

59.9±33.1% (n=6). However, Z944 did not prevent NAm activation by Epi (regular spiking (n=4/7) or burst firing (n=2/7) (**Figure 7D**), except in one of the regular spiking neurons tested (n=1/7). Therefore, while ICaT contributes to basal NAm neuronal excitability, it is not required for Epi-dependent NAm neuronal activation.

Persistent sodium current in NA neurons

We analyzed the prolonged sodium INaP current in adrenergic activation of Nam neurons. INaP is a slow inward current carried by voltage gated sodium channels, and contributes to spontaneous discharges in various cell types (Bevan and Wilson 1999; Koizumi and Smith 2008; Khaliq and Bean 2010, see Discussion). INaP was isolated as a TTX sensitive component of inward current that developed during a slow voltage ramp (+20 mV/s, **Figure 8A**). A large part of the INaP was highly sensitive to TTX (inhibited by 10nM TTX, 33.7±19.3 pA at -40 mV, n=5), while a significant current was carried by less TTX-sensitive channels (inhibited by 1µM TTX, 33.6±24.1 pA at -40 mV, n=5). The INaP was already present near the resting membrane potential of NAm neurons (**Figure 8A**), and continuously developed to peak at -10~0mV. Current with a similar I-V relationship was also isolated by applying the non-selective persistent sodium current inhibitor riluzole (30 µM, IC_{50} 2.3~51 µM (Zona, Siniscalchi et al. 1998; Wang, Lin et al. 2008), 33.1±32.9 pA at -40 mV, n=5, **Figure 8B**). At this concentration, riluzole was highly effective at preventing adrenergic activation of NAm neurons and fully prevented the increase of spontaneous AP discharges in all 5 NAm neurons tested (**Figure 8C**). Even in the presence of riluzole, AP's could still be evoked by local electrical stimulation, indicating that the observed effect is not due to a non-selective inhibition of sodium current. Since sodium channels are divided into classes based on their sensitivities to nano-molar TTX (Goldin 2001), we also examined whether TTX-sensitive or insensitive channels contribute to the adrenergic activation. Bath application of 10 nM TTX severely lowered the spontaneous AP rate of NAm neurons (80.9±26.3% reduction from baseline, n=5 **Figure 8D**). Under this condition, Epi was still able to increase AP firing rate in all five neurons tested (n=5/5, **Figure 8D**). Thus, while sodium channels that are highly sensitive to TTX carry a

majority of the INaP in NAm and are important for basal NAm excitability, TTX-insensitive sodium channels alone are sufficient for Epi-dependent AP increases in NAm neurons.

Finally, we examined the effectiveness of the non-selective sodium current inhibitor flecainide, an antiarrhythmic useful in the control of a variety of supraventricular cardiac tachyarrhythmias, including those bearing Scn5a mutations underlying Brugada Syndrome (Salvage, Chandrasekharan et al. 2017). Flecainide (20 µM) was partially effective at preventing AP induction, and blocked Epi activation in 3/5 cells tested. Thus in addition to multiple myocardial targets, including Nav1.5 channels in the septal conduction system and cardiac myocytes, this clinically used peripheral sodium channel blocker may also affect central vagal nerve activity.

Together these results suggest that adrenergic activation of NAm neurons requires a persistent sodium current, predominately mediated by sodium channels with low TTX-sensitivity.

Discussion

This study identifies a central adrenergic mechanism regulating preganglionic cardiac vagal neurons in the brainstem. We found that two adrenergic agonists, epinephrine and norepinephrine, significantly increase the spontaneous discharge rate of these neurons by acting at α1 and β receptors (**Figures 2&3**). This adrenergic activation, however, does not require synaptic transmission, since 1) it occurred even when the receptors were pharmacologically inhibited, and 2) following exposure, there was no significant change in the frequency of release at either excitatory and inhibitory synapses onto NAm neurons (**Figure 4**). Instead, we observed an increase in their intrinsic membrane excitability leading to vigorous rhythmic discharge (**Figures 5-8**). We also found that NAm neurons express functional hyperpolarization-activated current (Ih), T-type calcium current (ICaT), and persistent sodium (INaP) current, and of these, the INaP is critically required for intrinsic adrenergic activation. These results define a novel mechanism for central

adrenergic regulation of parasympathetic output to the heart, and provide a target excitatory mechanism of NAm preganglionic neuron rhythmic activity.

Catecholamines, especially epinephrine, are released in the circulation under stress, however their role at central sites is not commonly considered because of poor blood brain barrier permeability. Adrenergic neurons are located in the brainstem in proximity to NAm (e.g. A1, C1 groups), and are a likely source of synaptic regulation. Optogenetic activation of neurons within the C1 group in the medulla triggers mild bradycardia (Abbott, DePuy et al. 2013), and the adrenergic mechanism identified in this study may contribute in part to this effect. Given the preganglionic sympathetic roles of these catecholaminergic neurons, adrenergic co-activation of NAm neurons may counterbalance excessive cardiac sympathetic outflow to limit tachycardia. Alternatively, co-activation of cardiac sympathetic and parasympathetic pathway might increase the risk of arrhythmias such as atrial fibrillation (Inoue and Zipes 1987; Ogawa, Zhou et al. 2007).

Previous studies have suggested that adrenergic agonists can modulate cardiac vagal neurons by altering transmission of their afferent synapses. β-receptor agonists inhibit both sEPSCs and sIPSCs (Bateman, Boychuk et al. 2012), and α1 receptors inhibit IPSCs (Boychuk, Bateman et al. 2011). The α2 receptor agonist clonidine and dexmedetomidine inhibit sIPSC (Philbin, Bateman et al. 2010; Sharp, Wang et al. 2014). Finally, photostimulation of endogenous adrenergic fibers from locus coeruleus inhibited NAm neuronal discharge by selective augmentation of inhibitory currents (Wang, Pinol et al. 2014). Based on these reports, the relatively minor effect of adrenergic agonists on excitatory and inhibitory synaptic transmission onto NAm neurons in our preparation was not expected. The discrepancy in the magnitude of this effect could be explained by the 1) species differences (rat vs mouse), 2) the age of animals (neonate vs young adult), or 3) the precise recorded neuronal population (retrograde tracer labeling vs Chat-cre reporter). Among these, the age may play a significant role, since rodents show significant postnatal development of the parasympathetic autonomic regulatory system (Kasparov and Paton 1997) during the initial 3-weeks of life. In addition, we used thinner brain slices (200μm)

from the larger adult brainstem than the previous studies (500-600 µm) obtained from the smaller brainstem of younger animals where neuronal and synaptic density could be higher, leading to alternative estimates of the contribution of synaptic input.

In addition, the present studies reliably detected rebound APs (**Figure 5**) which were not reported in neonatal NAm neurons (Mendelowitz 1996; Mihalevich, Neff et al. 1996). Since rebound APs have been observed in adult guinea pig Nam neurons (Johnson and Getting 1991), there could be age-dependent development of this intrinsic membrane excitation mechanism. Alternatively, labeling with the lipophilic dye used for cardiac retrograde tracing used in previous studies (Mendelowitz 1996; Mihalevich, Neff et al. 1996) may have modified excitability of plasma membrane and masked the intrinsic membrane excitatory mechanism.

Characterizing NAm neuron subpopulations

We studied validated preganglionic NAm neurons based on their soma diameter, chat-tdtomato reporter expression, and colabeling with retrograde tracer. A previous study of NAm neurons in adult guinea pig brainstem, using sharp electrode intracellular recording (Johnson and Getting 1991), also identified multiple neuronal populations according to membrane excitability and cell size. Our recordings showing significant generation of delayed rebound action potentials are consistent with one population described in the earlier study. Although a detailed characterization of the other cell types was not conducted, it is likely that they are Chat-tdtomato^{+} non-preganglionic neurons (**Figure 1**) and Chat-tdtomato^{-} neurons. Further study of this population is warranted to confirm these identities and understand their contribution to cardiac regulation.

Our findings imply that the putative preganglionic NAm neurons can be further subdivided based on their response to adrenergic agonists; namely, neurons that show a simple increase in regular spiking and those that generate a burst discharge (**Figure 2**). Because of the low chance of encountering them, we could not characterize the burst firing neurons in further detail. Thus it is still unclear whether these two responses may represent two different intrinsic populations or a difference attributable to synaptic connectivity. However since

changes in intrinsic membrane excitability were consistently observed in all neurons tested (**Figure 5**), it is likely that enhancement of membrane excitability by adrenergic agonists affects both cell types.

Intrinsic excitation mechanisms of NAm neurons

Polyamines. The present study showed that intracellular dialysis-sensitive polyamines are likely to be an important regulator to maintain the excitability of NAm neurons (**Figure 5**). *In situ* hybridization studies in mouse brain indicate significant expressions of the spermine biosynthesis enzymes, ornithine decarboxylase (Odc1), spermidine synthase (Srm) and spermine synthase (Sms) in this brainstem region (**Supplementary Figure 1A**). While their molecular targets are not determined, one of the candidate mechanisms is an intracellular inhibition of inward rectifier potassium channels (Kir) (Ficker, Taglialatela et al. 1994; Lopatin, Makhina et al. 1994). Because Mg^{2+} ion is supplemented in the internal solution we used, the extent of a contribution by spermine is unclear, but block of Kir by spermine limits outward K^+ current, thereby maintaining membrane excitability. Further detailed characterization will elucidate this possibility.

Voltage-gated channels. A subset of NAm neurons possesses oscillatory membrane responses following recovery from hyperpolarizing voltage shifts, and using specific inhibitors, we confirmed that ICaT current contributes to generating this excitation pattern. Cav3.1 and Cav3.2 channels mRNA transcripts show local expression in NAm neurons (**Supplementary Figure 1B, Allan Brain Atlas**), and these channels may be responsible for the ICaT current. Hyperpolarizing current activates Ih current which is immediately followed by ICaT current-dependent rebound action potentials. In the presence of adrenergic agonists, this property could be further enhanced and could generate recurrent action potentials that can last for a few seconds (**Figure 7**). While these currents did not appear to contribute to the firing threshold for adrenergic activation of single spontaneous Aps in the *in vitro* preparation, these properties could be reflected in physiological processes such as vagal outflow during baroreflex and sustained vagal activity *in vivo*.

Our study suggests that INaP is critically involved in adrenergic activation of Nam neurons. A similar INaP mediated AP generation has been reported in hippocampal CA1 pyramidal neurons where INaP plays a critical role in muscarinic agonist-induced spontaneous AP generation (Yamada-Hanff and Bean 2013). The present study suggests that NAm neurons also possess a similar metabotropic agonist-dependent increase of spontaneous APs mediated by INaP. Our results also showed that NAm neurons express both TTX-sensitive (i.e. inhibited by 10nM TTX) and insensitive Na^+ currents, and that the TTX-insensitive sodium channels play an important role in adrenergic activation of NAm (**Figure 8**), similar to other neurons known to utilize Na current for pacemaking (Bevan and Wilson 1999; Mercer, Chan et al. 2007; Koizumi and Smith 2008; Khaliq and Bean 2010). TTX-insensitive channels are encoded by Scn5a (Nav1.5), Scn10a (Nav1.8), and Scn11a (Nav1.9), that generate currents with IC_{50} for TTX above 1 μM (Goldin 2001). These TTX insensitive channels are mostly expressed in cardiac and peripheral nerve system, and expression of these channels may contribute to unique excitation mechanism of NAm and may be unpurposefully affected by peripheral sodium channel blockers, such as flecainide.

While we do not yet know exactly which of the genes for ICaT and INaP contribute to the calcium and sodium currents in Nam neurons, modification of such channels may be exploited to regulate vagal regulation and severe mutation in the gene(s) could compromise vagal excitability and increase risk of cardiac arrhythmias. In addition to the voltage gated inward current, increased membrane resistance by adrenergic agonists suggests modification of potassium channels. Further elucidation of ionic current and responsible ion channels/transporters would provide insights into the genetics of parasympathetic cardiac regulation.

In summary, this study shows an adrenergic activation mechanism of NAm neurons mediated by modulation of intrinsic membrane excitability that requires INaP current. The results add an additional site of interaction between the sympathetic and parasympathetic systems within the medulla (DePuy, Stornetta et al. 2013), and may contribute to fine tuning central autonomic cardiovascular regulation.

Acknowledgments

We thank Dr Terry Snutch at the University of British Columbia for generously providing us with Z944. This study was supported by NIH/NINDS U01 NS090340 (JLN).

Figure Legends

Figure 1 Chat-tdtomato+ labeling of preganglionic neurons within the Nucleus Ambiguus (NAm). A&B Retrograde tracer DiO was injected into the pericardiac sac, and cells colabelled with retrograde dye and Chat-tdtomato fluorescence were analyzed. Low magnification (4x, scale bar: 1 mm, **A**) and higher magnification (20x, scale bar: 400 µm, **B**) images. DiO was detected mostly in cells with a large soma and was absent in the majority of small Chat-tdtomato^{+} cells (arrow heads), suggesting that most preganglionic cells are larger soma size. **C.** Unlabelled preganglionic and non-preganglionic Chat-tdtomato^{+} cells (threshold soma size 40µm) could be readily distinguished in acute brainstem slices prepared from young adult animals. **D-F**. Preganglionic neurons (n=100, soma diameter >40µm) and non-preganglionic (n=9) neurons showed distinct membrane excitability.

Figure 2 Adrenergic agonist activation of NAm neurons *in vitro*. A. Bath application of epinephrine (10µM) reversibly increased spontaneous action potential rate in silent (top) and spontaneous active (bottom) neurons. **B.** In some neurons (12%, 8/67 NAm cells), epinephrine modulated NAm firing in a burst suppression pattern. All of the burst neurons were spontaneously active. **C.** Summary data of basal spontaneous AP rate of recorded neurons (n=75). **D.** Comparison of AP frequency changes by Epi and NE exposures. Norepinephrine had a less potent excitatory effect (n=7 neurons).

Figure 3 α1 and β adrenergic receptors are required for adrenergic NAm activation. A, B&D. Bath application of β blocker (propranolol), α1 blocker (Doxazosin) and α1/β

dual antagonist (Carvedilol) prevented epinephrine-induced activation of NAm neurons. **C.** In 44% (4/9 cells) NAm neurons, a1 agonist phenylephrine alone could activate NAm neurons.

Figure 4 Adrenergic activation does not require synaptic mechanism. **A**. Inhibition of excitatory transmission by NBQX significantly reduced basal firing rate of NAm, but did not prevent activation by epinephrine. **B.** Similarly, inhibition of inhibitory synaptic transmission by Gabazine and strychnine did not prevent the adrenergic activation of NAm neurons. **C&D** NBQX and gabazine/strychnine cocktail used in these experiments fully eliminated spontaneous excitatory (sEPSC) and inhibitory currents (sIPSC), respectively. **E&F** Epinephrine or norepinephrine which induced spontaneous AP did not modify sEPSC or sIPSC frequency in the NAm neurons.

Figure 5 Modulation of intrinsic excitability by adrenergic stimulation. **A&B** Intracellular dialysis sensitivity of NAm neurons. Rebound discharge was highly sensitive to intracellular dialysis (**A**). This run-down effect could be reduced by inclusion of 0.5mM spermine (**B**). **C-E** epinephrine exposure significantly increased intrinsic membrane excitability of NAm neurons. **C.** adrenergic activation of a whole-cell clamp recorded NAm neurons. Voltage responses to step current injection (-200 pA+50 pA) in the same neurons in baseline (**D**) and after exposure to epinephrine (**E**). Note that measurements were made at -60mV to prevent generation of spontaneous action potentials. **F.** Membrane resistance changes before and after application of each adrenergic agonist. Control n=7. NE n=13, Epi n=10, *** $p<0.005$. **G.** Changes in evoked action potential numbers after NE or Epi application. No significant changes were detected. NE n=13, Epi n=10.

Figure 6 hyperpolarization activated current (Ih) is expressed but not required for adrenergic NAm activation. **A.** Ih mediated membrane sag during hyperpolarizing current was abolished by Ih inhibitor ZD7288 (10µM). **B.** ZD7288 did not prevent NAm activation by epinephrine.

Figure 7 Contribution of T-type Calcium current (ICaT) to the intrinsic membrane excitability of NAm neurons. **A.** Representative traces of the steady current inactivation of Isolated ICaT current of the NAm neuron. **B.** Summary plots of ICaT activation/inactivation kinetics. **C.** ICaT current inhibitor Z944 (1 µM) abolished rebound action potentials of NAm neurons. **D.** ICaT inhibition significantly reduced basal AP firing rate of NAm neurons, but did not fully prevent NAm activation by epinephrine.

Figure 8 Persistent sodium current (INaP) is required for the adrenergic activation of NAm neurons. **A&B** INaP in a NAm neuron. Slow voltage ramp (20 mV/s) triggered a small inward current which was partially inhibited by TTX (10 nM and 1 µM, **A**) and INaP inhibitor riluzole (**B**). **C.** Riluzole effectively prevented NAm activation by epinephrine. Note that riluzole did not prevent action potential (AP) evoked by electrical stimulation of surrounding tissue (arrows). **D.** A low concentration of TTX (10nM) reduced basal firing rate but did not fully prevent AP induction by epinephrine, suggesting expression and contribution of TTX-resistant Na^+ channels.

Supplementary Figure 1. *In situ* hybridization data from Allen Brain Atlas. **A.** Expression of genes involved in spermine biosynthesis in NA. Ornithine decarboxylase, structural 1 (Odc1) and Spermine synthase (Sms) showed dense labeling within the putative Nam (red arrows), while Spermidine synthase (Srm) expression is relatively sparsely distributed. **B.** Expression of genes encoding T-type calcium channels. CaV3.1 is distributed throughout the medulla while Cav3.2 showed dense labeling within the putative NAm.

References

Abbott, S. B., S. D. DePuy, et al. (2013). "Selective optogenetic activation of rostral ventrolateral medullary catecholaminergic neurons produces cardiorespiratory stimulation in conscious mice." J Neurosci **33**(7): 3164-3177.

Alboni, P., M. Alboni, et al. (2011). "Simultaneous occurrence of two independent vagal reflexes: a possible cause of vagal sudden death." Heart **97**(8): 623-625.

Bateman, R. J., C. R. Boychuk, et al. (2012). "beta adrenergic receptor modulation of neurotransmission to cardiac vagal neurons in the nucleus ambiguus." Neuroscience **210**: 58-66.

Bevan, M. D. and C. J. Wilson (1999). "Mechanisms underlying spontaneous oscillation and rhythmic firing in rat subthalamic neurons." J Neurosci **19**(17): 7617-7628.

Boychuk, C. R., R. J. Bateman, et al. (2011). "alpha1-adrenergic receptors facilitate inhibitory neurotransmission to cardiac vagal neurons in the nucleus ambiguus." Neuroscience **193**: 154-161.

Brailoiu, G. C., K. Benamar, et al. (2013). "Aldosterone increases cardiac vagal tone via G protein-coupled oestrogen receptor activation." J Physiol **591**(17): 4223-4235.

Byrum, C. E. and P. G. Guyenet (1987). "Afferent and efferent connections of the A5 noradrenergic cell group in the rat." J Comp Neurol **261**(4): 529-542.

Chemin, J., A. Monteil, et al. (2002). "Specific contribution of human T-type calcium channel isotypes (alpha(1G), alpha(1H) and alpha(1I)) to neuronal excitability." J Physiol **540**(Pt 1): 3-14.

Colman, N., K. Nahm, et al. (2004). "Epidemiology of reflex syncope." Clin Auton Res **14 Suppl 1**: 9-17.

DePuy, S. D., R. L. Stornetta, et al. (2013). "Glutamatergic neurotransmission between the C1 neurons and the parasympathetic preganglionic neurons of the dorsal motor nucleus of the vagus." J Neurosci **33**(4): 1486-1497.

Dergacheva, O., H. Kamendi, et al. (2009). "5-HT2 receptors modulate excitatory neurotransmission to cardiac vagal neurons within the nucleus ambiguus evoked during and after hypoxia." Neuroscience **164**(3): 1191-1198.

Dergacheva, O., A. Yamanaka, et al. (2016). "Direct projections from hypothalamic orexin neurons to brainstem cardiac vagal neurons." Neuroscience **339**: 47-53.

Dyavanapalli, J., P. Byrne, et al. (2013). "Activation of D2-like dopamine receptors inhibits GABA and glycinergic neurotransmission to pre-motor cardiac vagal neurons in the nucleus ambiguus." Neuroscience **247**: 213-226.

Ficker, E., M. Taglialatela, et al. (1994). "Spermine and spermidine as gating molecules for inward rectifier K+ channels." Science **266**(5187): 1068-1072.

Goldin, A. L. (2001). "Resurgence of sodium channel research." Annu Rev Physiol **63**: 871-894.

Inoue, H. and D. P. Zipes (1987). "Changes in atrial and ventricular refractoriness and in atrioventricular nodal conduction produced by combinations of vagal and sympathetic stimulation that result in a constant spontaneous sinus cycle length." Circ Res **60**(6): 942-951.

Irnaten, M., J. Wang, et al. (2001). "Firing properties of identified superior laryngeal neurons in the nucleus ambiguus in the rat." Neurosci Lett **303**(1): 1-4.

Jameson, H. S., R. A. Pinol, et al. (2008). "Purinergic P2X receptors facilitate inhibitory GABAergic and glycinergic neurotransmission to cardiac vagal neurons in the nucleus ambiguus." Brain Res **1224**: 53-62.

Johnson, S. M. and P. A. Getting (1991). "Electrophysiological properties of neurons within the nucleus ambiguus of adult guinea pigs." J Neurophysiol **66**(3): 744-761.

Johnson, S. M. and P. A. Getting (1992). "Excitatory effects of thyrotropin-releasing hormone on neurons within the nucleus ambiguus of adult guinea pigs." Brain Res **590**(1-2): 1-5.

Kalia, M., K. Fuxe, et al. (1985). "Rat medulla oblongata. III. Adrenergic (C1 and C2) neurons, nerve fibers and presumptive terminal processes." J Comp Neurol **233**(3): 333-349.

Kalla, M., N. Herring, et al. (2016). "Cardiac sympatho-vagal balance and ventricular arrhythmia." Auton Neurosci **199**: 29-37.

Kasparov, S. and J. F. Paton (1997). "Changes in baroreceptor vagal reflex performance in the developing rat." Pflugers Arch **434**(4): 438-444.

Khaliq, Z. M. and B. P. Bean (2010). "Pacemaking in dopaminergic ventral tegmental area neurons: depolarizing drive from background and voltage-dependent sodium conductances." J Neurosci **30**(21): 7401-7413.

Koizumi, H. and J. C. Smith (2008). "Persistent Na+ and K+-dominated leak currents contribute to respiratory rhythm generation in the pre-Botzinger complex in vitro." J Neurosci **28**(7): 1773-1785.

Koizumi, K. and M. Kollai (1981). "Control of reciprocal and non-reciprocal action of vagal and sympathetic efferents: study of centrally induced reactions." J Auton Nerv Syst **3**(2-4): 483-501.

Kvetnansky, R., E. L. Sabban, et al. (2009). "Catecholaminergic systems in stress: structural and molecular genetic approaches." Physiol Rev **89**(2): 535-606.

Lin, M., J. T. Hatcher, et al. (2011). "Maternal diabetes increases large conductance Ca2+-activated K+ outward currents that alter action potential properties but do not contribute to attenuated excitability of parasympathetic cardiac motoneurons in the nucleus ambiguus of neonatal mice." Am J Physiol Regul Integr Comp Physiol **300**(5): R1070-1078.

Loewy, A. D., S. McKellar, et al. (1979). "Direct projections from the A5 catecholamine cell group to the intermediolateral cell column." Brain Res **174**(2): 309-314.

Lopatin, A. N., E. N. Makhina, et al. (1994). "Potassium channel block by cytoplasmic polyamines as the mechanism of intrinsic rectification." Nature **372**(6504): 366-369.

Mendelowitz, D. (1996). "Firing properties of identified parasympathetic cardiac neurons in nucleus ambiguus." Am J Physiol **271**(6 Pt 2): H2609-2614.

Mercer, J. N., C. S. Chan, et al. (2007). "Nav1.6 sodium channels are critical to pacemaking and fast spiking in globus pallidus neurons." J Neurosci **27**(49): 13552-13566.

Mihalevich, M., R. A. Neff, et al. (1996). "Voltage-gated currents in identified parasympathetic cardiac neurons in the nucleus ambiguus." Brain Res **739**(1-2): 258-262.

Ogawa, M., S. Zhou, et al. (2007). "Left stellate ganglion and vagal nerve activity and cardiac arrhythmias in ambulatory dogs with pacing-induced congestive heart failure." J Am Coll Cardiol **50**(4): 335-343.

Perez-Reyes, E. (2003). "Molecular physiology of low-voltage-activated t-type calcium channels." Physiol Rev **83**(1): 117-161.

Perkins, K. L. (2006). "Cell-attached voltage-clamp and current-clamp recording and stimulation techniques in brain slices." J Neurosci Methods **154**(1-2): 1-18.

Philbin, K. E., R. J. Bateman, et al. (2010). "Clonidine, an alpha2-receptor agonist, diminishes GABAergic neurotransmission to cardiac vagal neurons in the nucleus ambiguus." Brain Res **1347**: 65-70.

Resch, J. M., H. Fenselau, et al. (2017). "Aldosterone-Sensing Neurons in the NTS Exhibit State-Dependent Pacemaker Activity and Drive Sodium Appetite via Synergy with Angiotensin II Signaling." Neuron **96**(1): 190-206 e197.

Salvage, S. C., K. H. Chandrasekharan, et al. (2017). "Multiple targets for flecainide action: implications for cardiac arrhythmogenesis." Br J Pharmacol.

Sharp, D. B., X. Wang, et al. (2014). "Dexmedetomidine decreases inhibitory but not excitatory neurotransmission to cardiac vagal neurons in the nucleus ambiguus." Brain Res **1574**: 1-5.

Shattock, M. J. and M. J. Tipton (2012). "'Autonomic conflict': a different way to die during cold water immersion?" J Physiol **590**(14): 3219-3230.

Stocker, S. D., B. C. Steinbacher, Jr., et al. (1997). "Connections of the caudal ventrolateral medullary reticular formation in the cat brainstem." Exp Brain Res **116**(2): 270-282.

Tringham, E., K. L. Powell, et al. (2012). "T-type calcium channel blockers that attenuate thalamic burst firing and suppress absence seizures." Sci Transl Med **4**(121): 121ra119.

Wang, X., R. A. Pinol, et al. (2014). "Optogenetic stimulation of locus ceruleus neurons augments inhibitory transmission to parasympathetic cardiac vagal neurons via activation of brainstem alpha1 and beta1 receptors." J Neurosci **34**(18): 6182-6189.

Wang, Y. J., M. W. Lin, et al. (2008). "Riluzole-induced block of voltage-gated Na+ current and activation of BKCa channels in cultured differentiated human skeletal muscle cells." Life Sci **82**(1-2): 11-20.

Yamada-Hanff, J. and B. P. Bean (2013). "Persistent sodium current drives conditional pacemaking in CA1 pyramidal neurons under muscarinic stimulation." J Neurosci **33**(38): 15011-15021.

Zona, C., A. Siniscalchi, et al. (1998). "Riluzole interacts with voltage-activated sodium and potassium currents in cultured rat cortical neurons." Neuroscience **85**(3): 931-938.

Figure 1

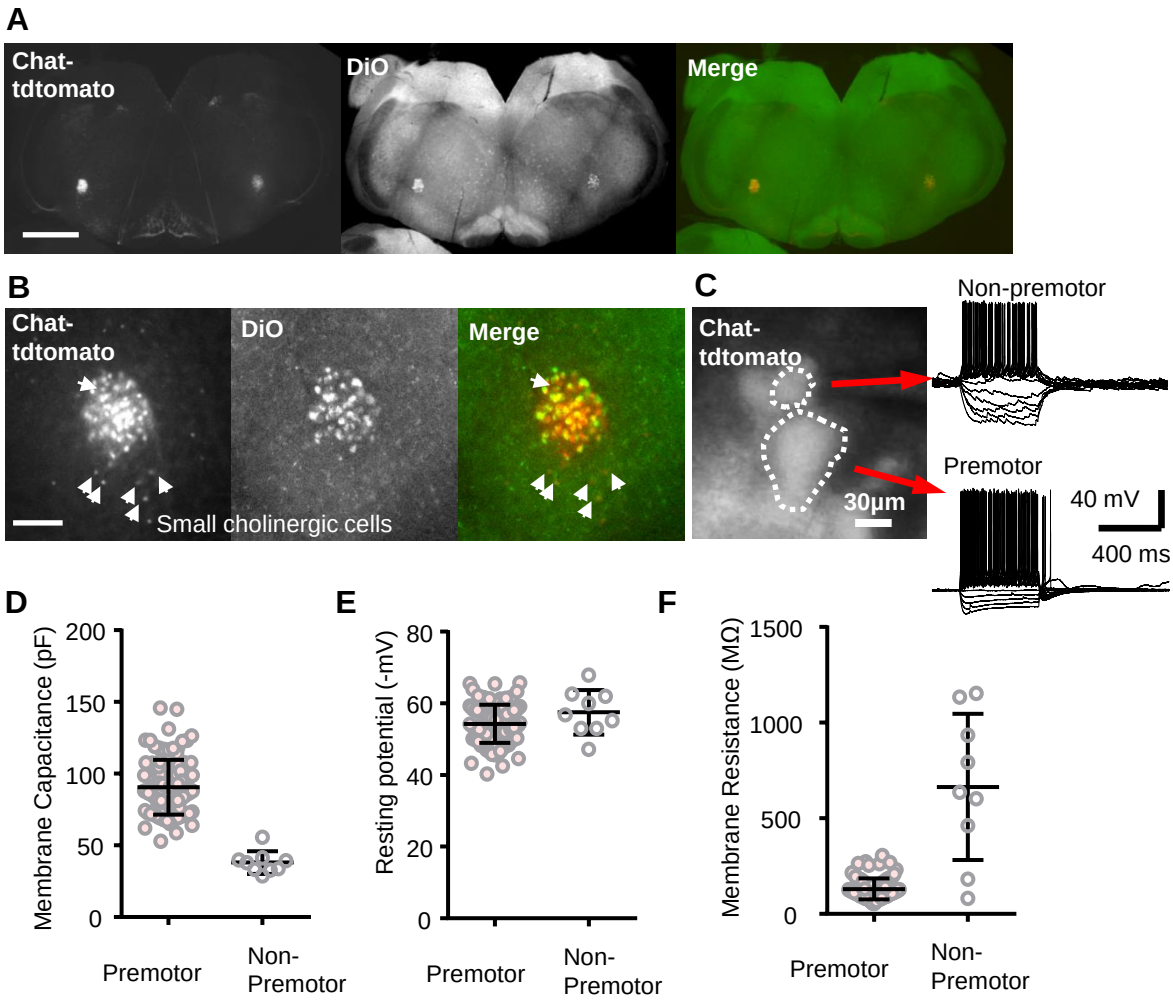
A
Chat-
tdtomato
DiO
Merge
B
Chat-
tdtomato
DiO
Merge
Small cholinergic cells
C
Chat-
tdtomato
30µm
Non-premotor
Premotor
40 mV
400 ms
D
Membrane Capacitance (pF)
200
150
100
50
0
Premotor
Non-
Premotor
E
Resting potential (-mV)
80
60
40
20
0
Premotor
Non-
Premotor
F
Membrane Resistance (MΩ)
1500
1000
500
0
Premotor
Non-
Premotor

Figure 2

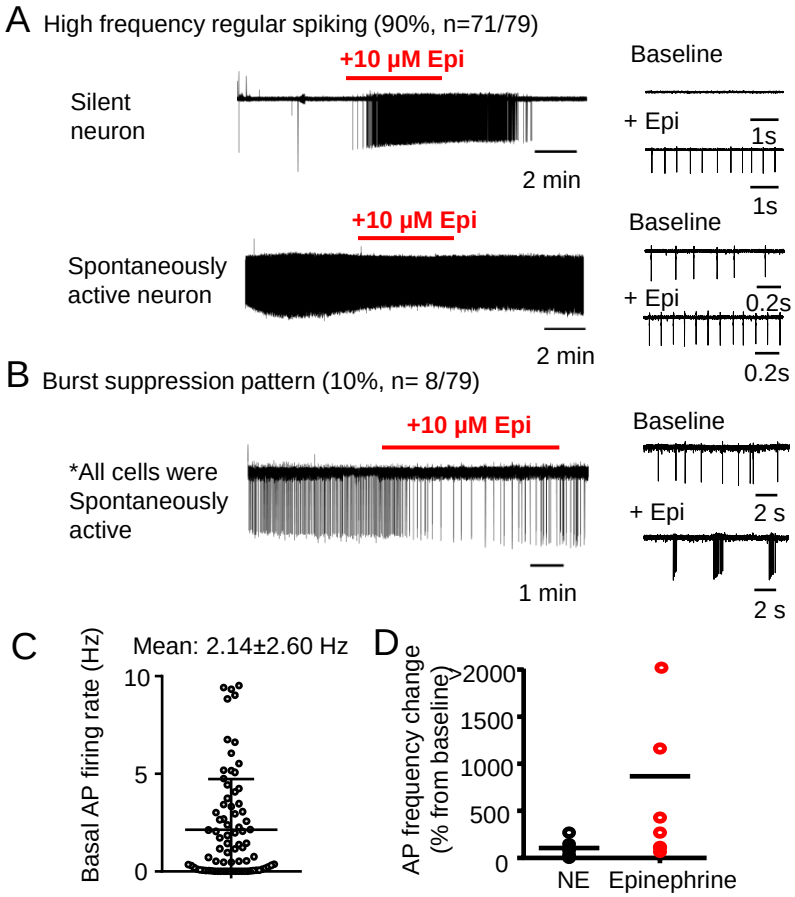
A High frequency regular spiking (90%, n=71/79)
+10 μM Epi
Silent neuron
2 min
Baseline
+ Epi
1s
1s
+10 μM Epi
Spontaneously active neuron
2 min
Baseline
+ Epi
0.2s
0.2s
B Burst suppression pattern (10%, n= 8/79)
+10 μM Epi
*All cells were Spontaneously active
1 min
Baseline
+ Epi
2 s
2 s
C
Mean: 2.14±2.60 Hz
Basal AP firing rate (Hz)
10
5
0
D
AP frequency change (% from baseline)
2000
1500
1000
500
0
NE
Epinephrine

Figure 3

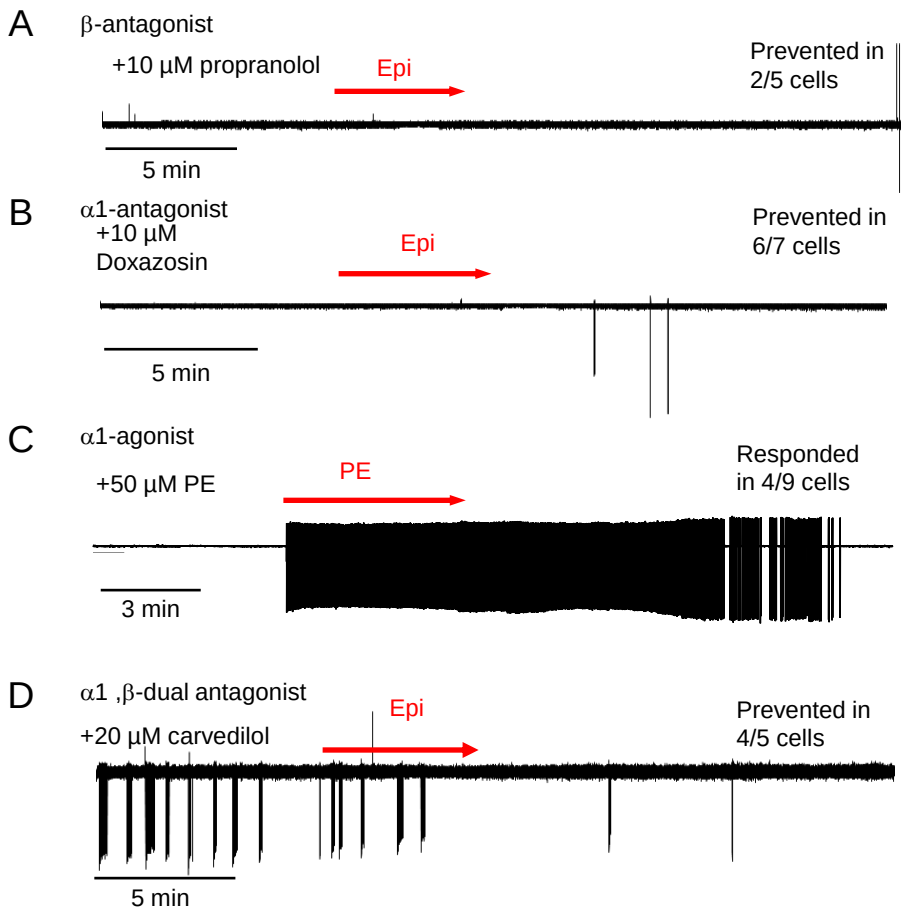
A
β-antagonist
+10 μM propranolol
Epi
Prevented in
2/5 cells
5 min
B
α1-antagonist
+10 μM
Doxazosin
Epi
Prevented in
6/7 cells
5 min
C
α1-agonist
+50 μM PE
PE
Responded
in 4/9 cells
3 min
D
α1 ,β-dual antagonist
+20 μM carvedilol
Epi
Prevented in
4/5 cells
5 min

Figure 4

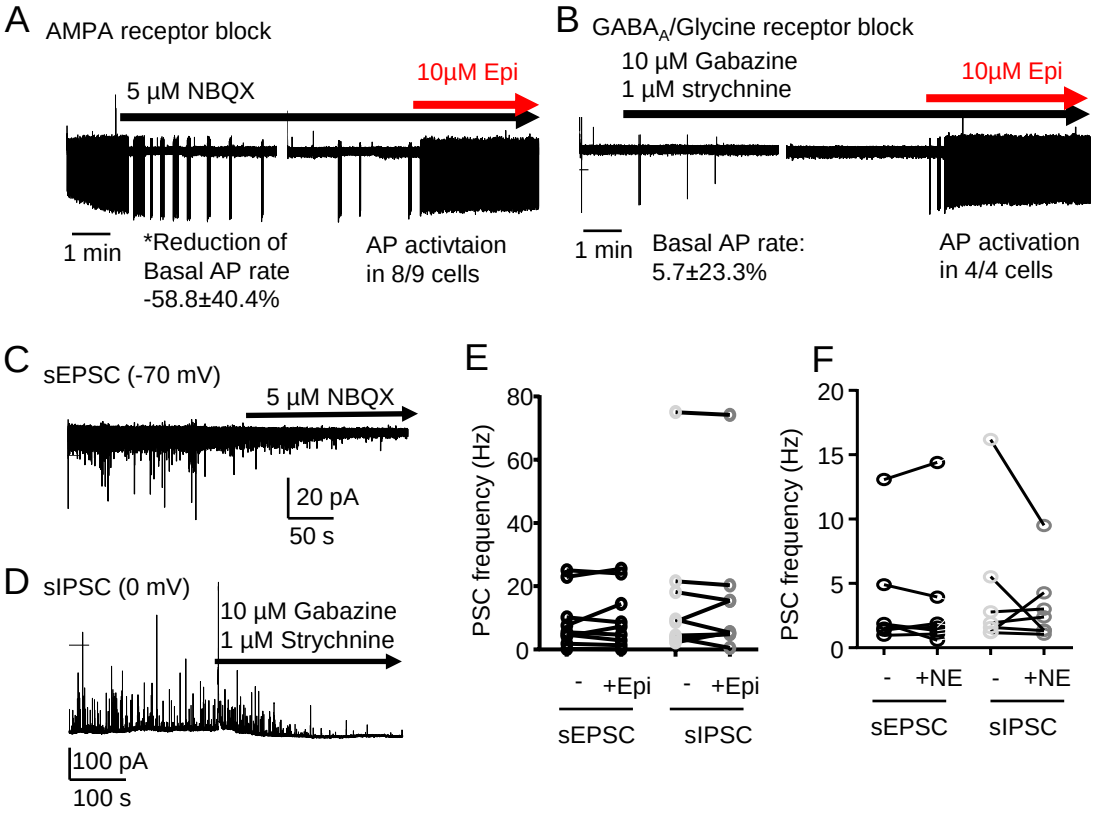
A
AMPA receptor block
5 µM NBQX
10µM Epi
1 min
*Reduction of
Basal AP rate
-58.8±40.4%
AP activtaion
in 8/9 cells
B
GABA$_A$/Glycine receptor block
10 µM Gabazine
1 µM strychnine
10µM Epi
1 min
Basal AP rate:
5.7±23.3%
AP activation
in 4/4 cells
C
sEPSC (-70 mV)
5 µM NBQX
20 pA
50 s
D
sIPSC (0 mV)
10 µM Gabazine
1 µM Strychnine
100 pA
100 s
E
PSC frequency (Hz)
80
60
40
20
0
-
+Epi
-
+Epi
sEPSC
sIPSC
F
PSC frequency (Hz)
20
15
10
5
0
-
+NE
-
+NE
sEPSC
sIPSC

Figure 5

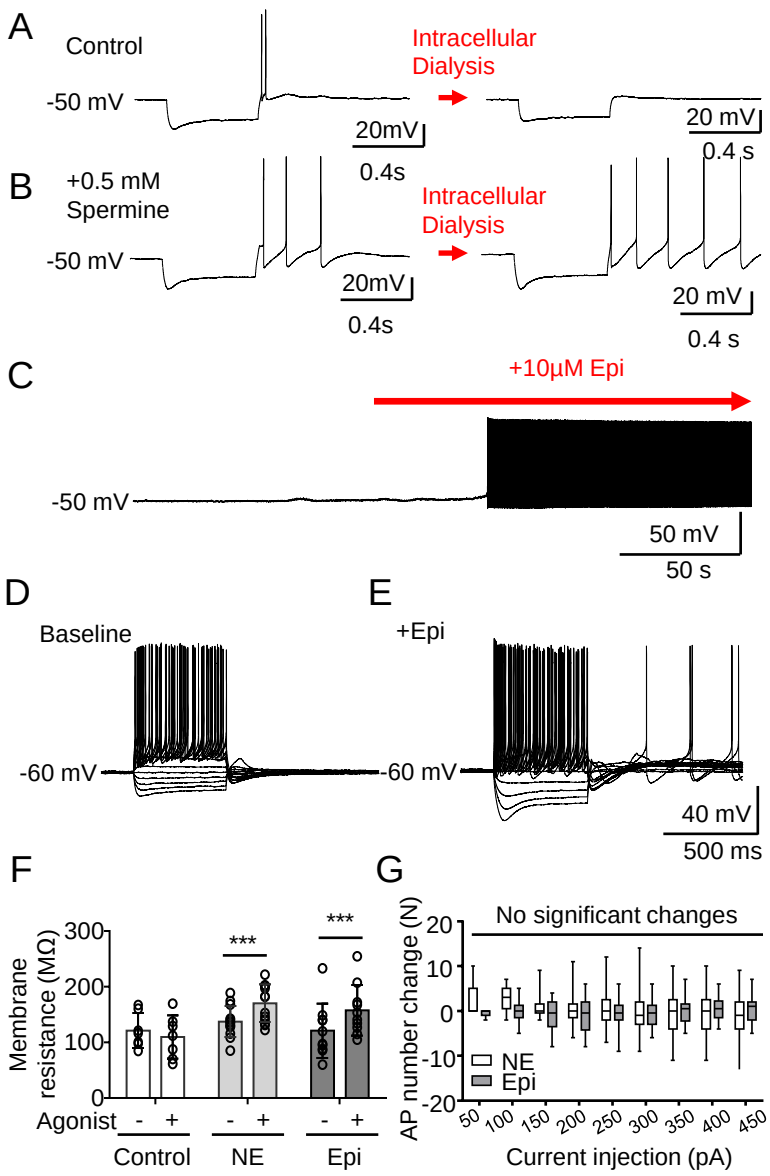
A
Control
-50 mV
Intracellular
Dialysis
20mV
0.4s
20 mV
0.4 s
B
+0.5 mM
Spermine
-50 mV
Intracellular
Dialysis
20mV
0.4s
20 mV
0.4 s
C
+10µM Epi
-50 mV
50 mV
50 s
D
Baseline
-60 mV
E
+Epi
-60 mV
40 mV
500 ms
F
Membrane
resistance (MΩ)
300
200
100
0
***
***
Agonist
-
+
-
+
-
+
Control
NE
Epi
G
No significant changes
AP number change (N)
20
10
0
-10
-20
NE
Epi
50
100
150
200
250
300
350
400
450
Current injection (pA)

Figure 6

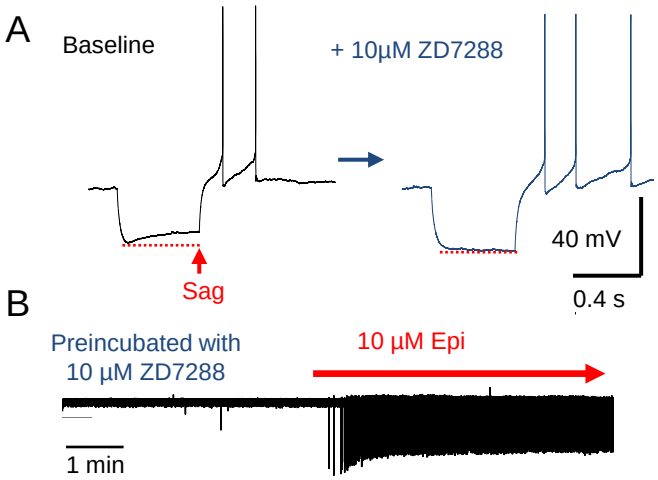
A
Baseline
+ 10μM ZD7288
Sag
40 mV
0.4 s
B
Preincubated with
10 μM ZD7288
10 μM Epi
1 min

Figure 7

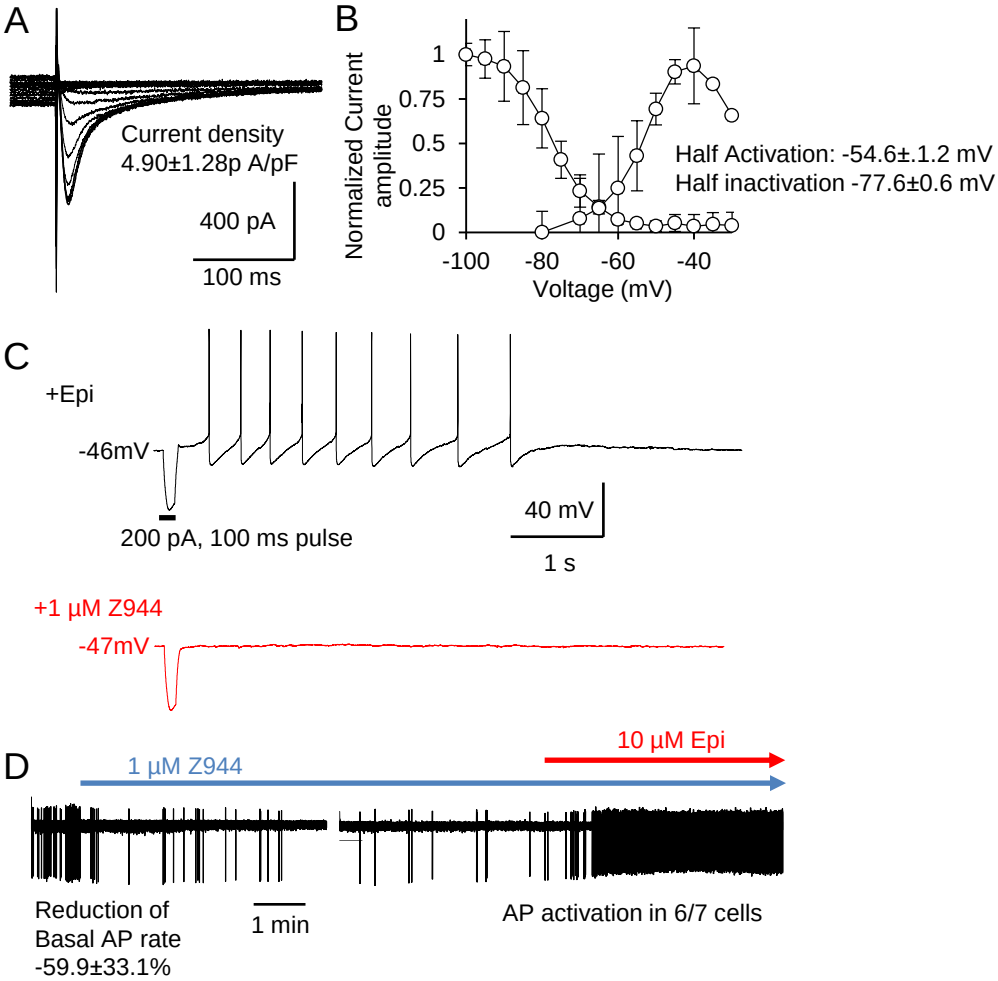
A
Current density
4.90±1.28p A/pF
400 pA
100 ms
B
Normalized Current amplitude
1
0.75
0.5
0.25
0
-100
-80
-60
-40
Voltage (mV)
Half Activation: -54.6±.1.2 mV
Half inactivation -77.6±0.6 mV
C
+Epi
-46mV
200 pA, 100 ms pulse
40 mV
1 s
+1 µM Z944
-47mV
D
1 µM Z944
10 µM Epi
Reduction of
Basal AP rate
-59.9±33.1%
1 min
AP activation in 6/7 cells

Figure 8

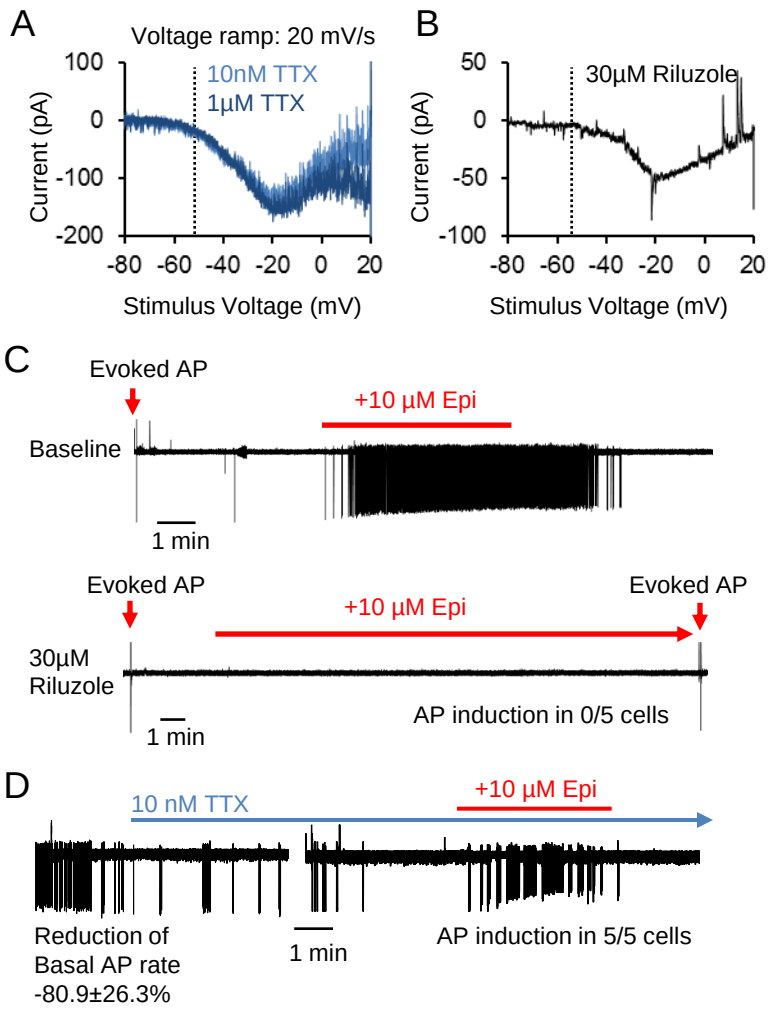
A
Voltage ramp: 20 mV/s
10nM TTX
1μM TTX
Current (pA)
100
0
-100
-200
-80 -60 -40 -20 0 20
Stimulus Voltage (mV)
B
30μM Riluzole
Current (pA)
50
0
-50
-100
-80 -60 -40 -20 0 20
Stimulus Voltage (mV)
C
Evoked AP
+10 μM Epi
Baseline
1 min
Evoked AP
+10 μM Epi
Evoked AP
30μM
Riluzole
1 min
AP induction in 0/5 cells
D
10 nM TTX
+10 μM Epi
Reduction of
Basal AP rate
-80.9±26.3%
1 min
AP induction in 5/5 cells

Supplementary Figure 1

In situ hybridization data from Allan brain atlas

A Spermine biosynthesis enzymes

ornithine decarboxylase, structural 1 (Odc1)

Spermidine synthase (Srm)

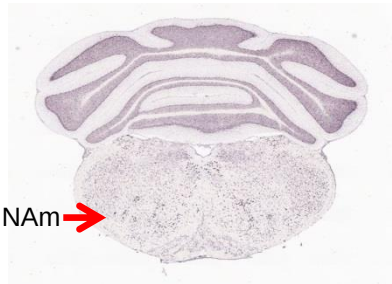

Spermine synthase (Sms)

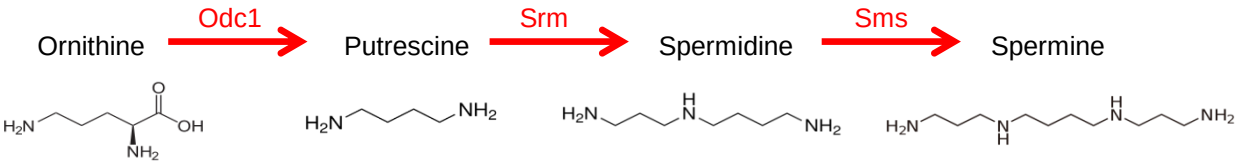

B T-type calcium channels

Cav3.1

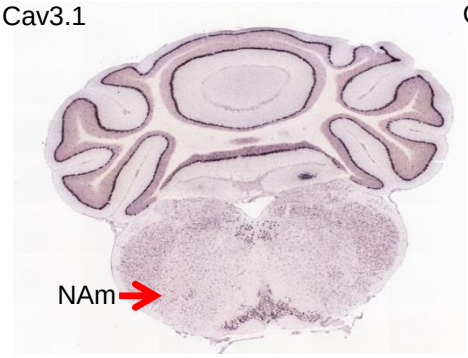
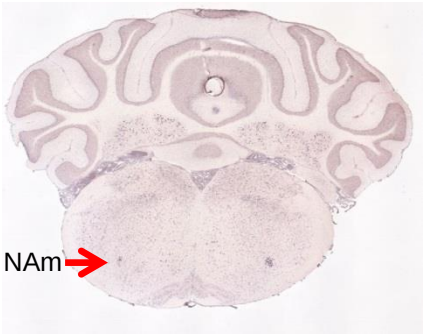
Cav3.2